

# Investigating and Optimizing the Chiral Properties of Lattice Fermion Actions

Thomas DeGrand, Anna Hasenfratz, and Tamás G. Kovács  
Physics Department, University of Colorado,  
Boulder, CO 80309 USA

(the MILC collaboration)

## Abstract

We study exceptional modes of both the Wilson and the clover action in order to understand why quenched clover spectroscopy suffers so severely from exceptional configurations. We show that, in contrast to the case of the Wilson action, a large clover coefficient can make the exceptional modes extremely localized and thus very sensitive to short distance fluctuations. We describe a way to optimize the chiral behavior of Wilson-type lattice fermion actions by studying their low energy real eigenmodes. We find a candidate action, the clover action with fat links with a tuned clover term. We present a calculation of spectroscopy and matrix elements at Wilson gauge coupling  $\beta = 5.7$ . When compared to simulations with the standard (nonperturbatively improved) clover action at small lattice spacing, the action shows good scaling behavior, with an apparent great reduction in the number of exceptional configurations.

# 1 Introduction

There is an increasing accumulation of evidence from lattice simulations of the importance of the topological properties of the QCD vacuum [1, 2]. Simulations of the pure gauge theory find that the vacuum is filled with instantons of size 0.3-0.5 fm, with a density of about one per  $\text{fm}^{-4}$ , although the precise numbers are still controversial [3, 4]. An elaborate phenomenology of the properties of hadrons is based on instanton dynamics and its connection to chiral symmetry breaking [5]. The extent to which the complete continuum phenomenology of instanton effects in hadronic physics is actually realized by QCD, and can be studied using lattice simulations, remains an open question, but its outline is present.

Lattice artifacts associated with instantons also seem to be connected to some of the difficulties of numerical simulations with quenched QCD, namely, eigenmodes of the Dirac operator which occur away from the critical quark mass, and which spoil the calculation of the fermion propagator, the so-called “exceptional configurations” [6]. Precisely how does this occur? And, given that instantons are responsible for chiral symmetry breaking, is it possible to optimize the lattice discretization of a fermion action with respect to its topological properties? Our goal is to shrink the range of bare quark mass over which the low lying real eigenmodes of the Dirac operator occur, on background gauge field configurations which are typical equilibrium configurations at some gauge coupling.

A chiral improvement of the lattice Dirac operator is expected to decrease the additive mass renormalization of zero-modes as well as their spread. This is indeed the case for classically perfect actions which have been proven to have exact zero modes with no shift or spread at all [7]. On the other hand, surprisingly, this does not seem to be true for the simplest improvement on the Wilson action, the clover action. Although the clover term reduces the additive mass renormalization as compared to the Wilson action, the problem with exceptional configurations appears to be more severe for the clover than for the Wilson action; at least with the non-perturbatively determined value of the clover coefficient  $C_{sw}$  [8]. On a set of 50  $12^3 \times 24$   $\beta = 5.9$  configurations the Fermilab group found 7 exceptional modes both with the Wilson and the clover action ( $C_{sw} = 1.91$ ) but the spread of the clover modes in terms of the pion mass was at least twice that of the Wilson modes. This indicates that surprisingly, improving the action makes the situation worse for exceptional configurations. In the present paper we show why this happens by studying how the real modes of the Dirac operator change with the clover coefficient.

We are then drawn to an alternate action, a modified clover action, where

the gauge connections are replaced by APE-blocked [9] links, and the clover coefficient  $C_{sw}$  is tuned to optimize chiral properties. Specifically,

$$\begin{aligned}
S &= \sum_n (m+4)\bar{\psi}(n)\psi(n) \\
&- \frac{1}{2} \sum_{n\mu} (\bar{\psi}(n)(1-\gamma_\mu)V_\mu(n)\psi(n+\mu) + \bar{\psi}(n)(1+\gamma_\mu)V_\mu^\dagger(n-\mu)\psi(n-\mu)) \\
&+ \frac{C_{sw}}{2} \sum_{n,\mu,\nu} \bar{\psi}(n)i\sigma_{\mu\nu}P_{\mu\nu}(n)\psi(n)
\end{aligned} \tag{1}$$

with

$$\begin{aligned}
V_\mu^{(n)}(x) &= (1-\alpha)V_\mu^{(n-1)}(x) \\
&+ \frac{\alpha}{6} \sum_{\nu \neq \mu} (V_\nu^{(n-1)}(x)V_\mu^{(n-1)}(x+\hat{\nu})V_\nu^{(n-1)}(x+\hat{\mu})^\dagger \\
&+ V_\nu^{(n-1)}(x-\hat{\nu})^\dagger V_\mu^{(n-1)}(x-\hat{\nu})V_\nu^{(n-1)}(x-\hat{\nu}+\hat{\mu})),
\end{aligned} \tag{2}$$

with  $V_\mu^{(n)}(x)$  projected back onto  $SU(3)$  after each step, and  $V_\mu^{(0)}(n) = U_\mu(n)$  the original link variable. We take  $\alpha = 0.45$  and  $N = 10$  smearing steps, chosen because of our previous work on instantons [3]. This choice of parameters is not unique and might not even be optimal.  $P_{\mu\nu}$  is the usual clover set of links, but built of the  $V_\mu$ 's. At Wilson gauge coupling  $5.7 - 5.8$ , the best choice is  $C_{sw} = 1.2$ , and it decreases to the tree-level  $C_{sw} = 1$  value at larger  $\beta$ . We will also quote simulation data in terms of the hopping parameter,  $\kappa = 1/(8+2m)$ .

The optimized action has a spread of low lying real eigenmodes with respect to the bare quark mass which is less than a third of the spread for the usual Wilson action. In terms of the square of the pion mass the spread is about three times smaller for the optimized action than for the standard Wilson action. The action has other good features, as well: the renormalization factors connecting lattice quantities to their continuum values appear to be very close to unity. The action also appears to require only about half the number of sparse matrix inversion steps as the usual clover action (at equivalent values of the physical parameters).

The action we propose is completely unimproved in its kinetic properties, so its dispersion relation and heavy quark mass artifacts are identical to those of the Wilson action. It would be very easy to improve it by beginning with a more complicated free fermion discretization.

Fermion actions with fat links have received considerable attention in the past year. The first use of them we know of (although with a different motivation) was in the simulations of QCD on cooled gauge fields by the MIT group [10]. The MILC collaboration [11], Orginos and Toussaint [12] and Lagaë and

D. K. Sinclair[13] have shown that modest fattening considerably improves flavor symmetry restoration in simulations with staggered fermions. We have used calculations of staggered spectroscopy on highly smoothed gauge configurations to compare chiral symmetry breaking in  $SU(2)$  gauge theory and in instanton backgrounds [14]. Finally, all fixed point actions and approximate fixed point actions we know of [15, 16] for fermions seem to incorporate fat links. Fixed point fermions realize the index theorem and retain chiral symmetry at nonzero lattice spacing [7], and so one way of viewing a fat link action is as an approximate FP action, which includes its chiral properties but not its kinetic ones.

An apparent drawback of fat link actions is the lack of a transfer matrix between consecutive time slices.  $N$  APE steps can mix links up to  $\pm N$  timeslices away and a strict transfer matrix cannot be defined on time slices closer than  $2N$  lattice spacings (20 in our case). In practice we are concerned only with the exponential decay of correlation functions and we found asymptotic decay after 2-5 time slices in our simulation. This is expected if we realize that APE smearing is basically a random walk whose range can be estimated as  $\sqrt{N}\alpha \approx 1.4$  in our case.

The outline of the paper is as follows: In Section 2 we review the continuum index theorem and describe how lattice fermions fail to reproduce it. We then describe how we find the real eigenmodes of the Wilson-Dirac operator. All this is basically a review, and experts may skip it. In Section 3 we describe the connection between small topological objects and exceptional configurations for the thin-link clover action. In Section 4 we return to the fat link clover action and describe the tests we performed to tune the action. Section 5 describes a calculation of spectroscopy and matrix elements at  $aT_c = 1/4$  (Wilson gauge coupling  $\beta = 5.7$ ) using the new action.

## 2 Measuring the Chiral Properties of Wilson-like Fermions

The reader might recall that in the continuum the local topological density

$$q(x) = \frac{1}{32\pi^2} \epsilon_{\mu\nu\rho\sigma} F_{\mu\nu} F_{\rho\sigma} \quad (3)$$

is related to the divergence of the flavor singlet (with  $n_f$  flavors) axial-vector current

$$\partial_\mu \bar{\psi} i \gamma_\mu \gamma_5 \psi = 2m \bar{\psi} i \gamma_5 \psi + 2in_f q. \quad (4)$$

Integrating over all  $x$ , this relation implies a connection between the topological charge  $Q = \int d^4x q(x)$  and a mode sum,

$$Q = m \text{Tr} \bar{\psi} \gamma_5 \psi = m \text{Tr} \gamma_5 \frac{1}{\gamma \cdot D + m} = m \sum_s \frac{f_s^\dagger \gamma_5 f_s}{i\lambda_s + m} \quad (5)$$

where  $f_s$  are the eigenfunctions of the (antihermitian) Dirac operator  $\gamma \cdot D$ ,  $\gamma \cdot D f_s = i\lambda_s f_s$ , with  $\lambda_s$  real. The property  $\{\gamma_5, \gamma \cdot D\} = 0$  leads to the condition that  $f_s^\dagger \gamma_5 f_s = 0$  if  $\lambda_s \neq 0$ , and if  $\lambda_s = 0$  we may choose  $f_s$  to have a definite chirality,  $\gamma_5 f_s = \pm f_s$ . Thus it follows that

$$Q = \sum_{s, \lambda_s=0} f_s^\dagger \gamma_5 f_s = n_+ - n_- \quad (6)$$

where  $n_+$  and  $n_-$  are the number of zero eigenmodes with positive and negative chirality. This is the index theorem.

On the lattice, essentially every statement in the preceding paragraph is contaminated by lattice artifacts [17]. Here we focus on Wilson-like fermions, where chiral symmetry is broken by the addition of terms proportional to the Dirac scalar and/or tensor operators. The Wilson or clover fermion action analog of  $\gamma \cdot D$ ,  $D_w$ , is neither Hermitian nor antihermitian and its eigenvalues are generally complex.  $D_w$  can also have real eigenvalues. These real eigenvalues usually do not occur at zero. Their locations spread around  $-m_c$  where  $m_c$  is the critical bare mass, at which the pion mass vanishes. For Wilson-like fermions  $m_c$  is usually negative and its magnitude decreases with increasing clover term.

On smooth, isolated instanton background configurations, the location of the real eigenmode varies with the size  $\rho$  of the instanton. For large instantons, the low lying real mode occurs close to zero. Accompanying this near-zero mode, there is a set of modes which do not cluster around zero, but around  $\simeq O(1)$  (in lattice units). These are ‘‘doubler modes.’’ As one decreases the instanton size, the eigenmode near zero shifts in the positive direction, approaching the doubler modes. This  $\rho$ -dependent mass shift and the location of the doubler modes all depend on the particular choice of lattice fermion action [18, 19]. The shift of the low lying real eigenmode for a given instanton size for the Wilson action is larger than for the clover action, which has better chiral properties. Nevertheless, for both actions, as the instanton size decreases, sooner or later the lowest eigenvalue starts to increase, approaches the doublers and eventually annihilates with one of the doublers - the fermion does not see the instanton any longer.

Real eigenmodes of the Dirac operator also occur on equilibrium background configurations. Typically, they occur around some average value, an overall  $\beta$ -dependent mass shift. The real eigenmodes also sense the topological content

of the background configuration and their positions can sometimes be correlated with the sizes of the background instantons. This is illustrated in Fig. 1 for the Wilson action, where we show the instanton size versus the corresponding fermionic eigenvalue both for smooth instantons and instantons identified on real Monte Carlo generated configurations at  $\beta = 6.0$  on  $12^4$  lattices. The instanton sizes were measured using the method of Ref. [3] and the real modes were extracted as described below. To find the corresponding instanton for each real mode, we compared the quark density of the given mode to the profile of the charge density. Usually the quark density had a well identifiable lump sitting exactly on an (anti)instanton. These lattices are fairly small in physical units with volumes  $V \simeq 2 \text{ fm}^4$  and contain on average about two topological objects. In some cases, however, these modes were peaked at not only one instanton, but more, and sometimes the quark density was so spread out that it was hard to identify a well defined peak. Fig. 1 contains results only from uniquely identifiable modes.

In addition to the low lying modes there are also doublers. Again there are two issues: First, do the low lying modes separate from the doubler modes, and second, what is the spread of the low lying modes.

The first question is important because, if the low lying modes do not separate from the doubler modes, then the physics of chiral symmetry breaking with a lattice cutoff is different than in the continuum. The lattice theory is no longer an approximation to the continuum, and one cannot speak of chiral symmetry breaking as being induced by instantons. Chiral symmetry is certainly broken in QCD for any value of the cutoff, including the strong coupling limit [21], but the mechanism does not involve instantons.

Note that if the low lying modes do not separate from the doubler modes, it does not make sense to talk about the spread of the low lying modes either.

The determination of the real eigenvalues  $\lambda$  of  $D_w$  is equivalent to computing the bare mass values  $m_\lambda = -\lambda$ , where the quark propagator  $(D_w + m)$  becomes singular. In the remainder of the present paper instead of the eigenvalue, we shall always quote the corresponding bare mass value, where the propagator is singular. On any particular background gauge configuration this can be computed very simply. We approximate

$$P(m) = \langle \bar{\psi} \gamma_5 \psi \rangle = \text{Tr}(D_w + m)^{-1} \gamma_5 \quad (7)$$

with a noisy estimator: cast a random vector  $\eta_i$  on each site  $i$ , solve  $(D_w + m)\chi = \eta$  for  $\chi$  and measure

$$P(m)_\eta = \sum_{ij} \text{Tr} \bar{\eta}_i \gamma_5 \chi_j \quad (8)$$

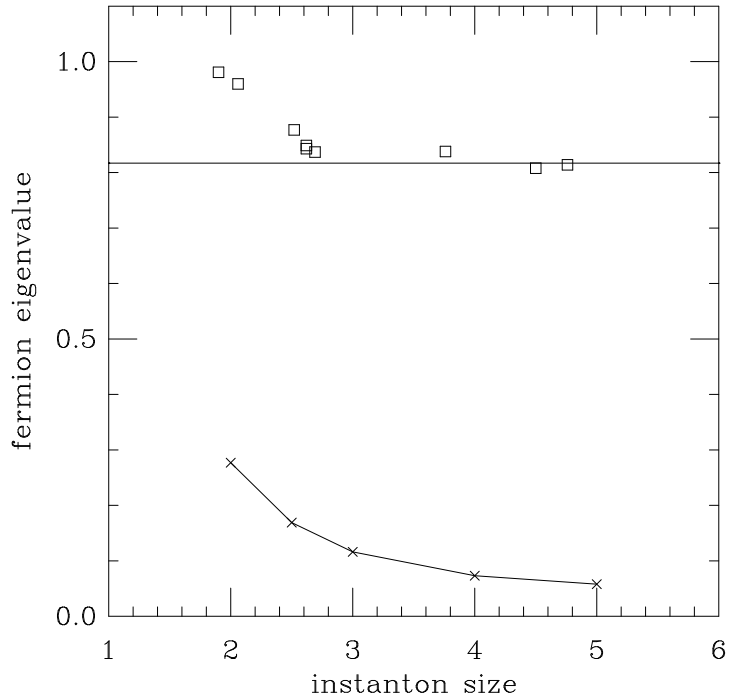


Figure 1: The instanton size (in units of the lattice spacing) vs. the eigenvalue of the corresponding (Wilson action) fermionic real mode on smooth instantons (crosses) and on real Monte Carlo generated configurations at  $\beta = 6.0$  (squares). The horizontal line indicates  $-m_c$  for the  $\beta = 6.0$  quenched ensemble.

as a function of  $m$ . If an eigenmode of  $D_w$  is located at  $\lambda$ , its presence is signaled by the appearance of a pole in  $P(m)$  at  $m = -\lambda$ . This is a variant on the standard method of measuring  $\langle \bar{\psi}\psi \rangle$  in a lattice simulation. It has also seen considerable use by the Fermilab group [6] in their studies of exceptional configurations (they use a flat source  $\eta_i = \text{constant}$ , not a noisy source). The eigenfunction itself of a particular mode can be found by performing the inversion for a test mass very close to the given pole. Then  $(D + m)^{-1}$  projects out

the corresponding eigenmode from the source. In this case  $\chi^\dagger\chi$  is (proportional to) the probability density for that mode. For computing the probability density we used a flat source rather than a random one.

### 3 Trouble with the Thin Link Clover Action

As we have seen in Fig. 1, on fine enough lattices with the Wilson action there is a strong correlation between the instanton size and the eigenvalue of the corresponding fermionic real mode; (near) exceptional modes correspond to large instantons. We shall now explore what happens in the presence of the clover term. We start by looking at smooth single instanton configurations. Our naive expectation is that since the clover term is designed to improve the chiral properties of the action, its inclusion should make the fermion modes more “continuum-like”. In other words, it should move the modes corresponding to different instanton sizes closer to one another and also shift them all towards zero. This is indeed what happens. In Fig. 2 we plot how the fermion eigenvalues associated with instantons of various sizes change as a function of the clover coefficient. For better legibility in the figure we include only the range of  $C_{sw} \geq 1.0$ . For the Wilson action ( $C_{sw} = 0$ ) the eigenvalues corresponding to instantons of size  $1.2 \leq \rho \leq 2.5$  are spread between 0.19 and 0.86.

As  $C_{sw}$  increases from zero to the tree level value,  $C_{sw} = 1$ , all the modes move closer to zero and their spread decreases. If  $C_{sw}$  is further increased, the modes start to pass through zero and also the trajectories corresponding to instantons of different sizes start to cross one another. By  $C_{sw} = 1.4$  the order of all the eigenvalues for instanton sizes  $\geq 1.5a$  has been reversed. As  $C_{sw}$  is increased, modes of smaller and smaller instantons cross over to the other side of the distribution.

What happens on equilibrium Monte Carlo configurations? We first performed a detailed study of the Fermilab quenched  $\beta = 5.9$  exceptional configurations reported in Ref. [6]. We determined the wave function of both the seven Wilson and the seven clover exceptional modes together with the instanton content of the corresponding background gauge configurations. Whereas in most of the cases the Wilson modes were sitting on a single large instanton, the clover modes were always spread over several topological objects.

This suggests that the mechanism responsible for the exceptional configurations might be different for the Wilson and the clover action. If indeed there is such a difference, we expect it to be more pronounced on coarser lattices, where exceptional configurations are more of a problem and also the clover coefficient

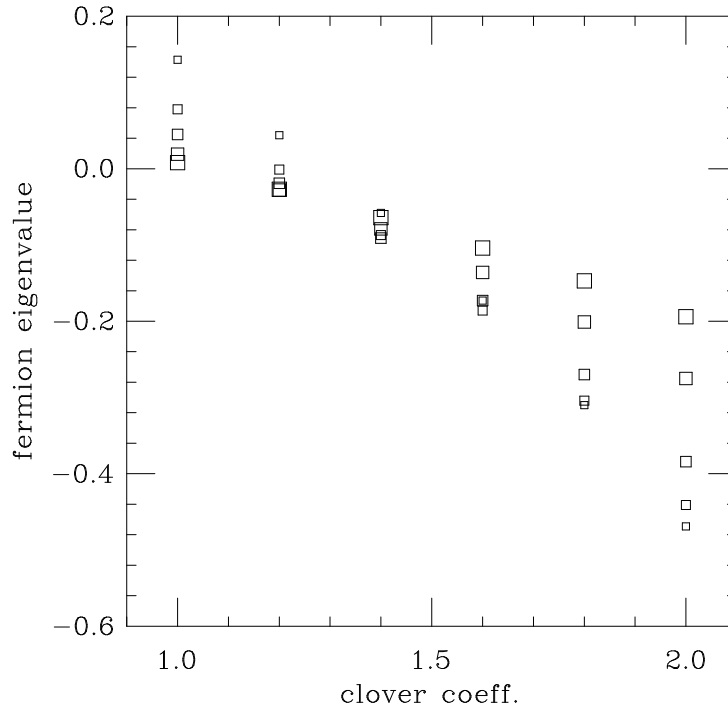


Figure 2: The real fermionic eigenvalue of the clover action versus the clover coefficient on instantons of sizes  $\rho/a = 1.2, 1.4, 1.6, 2.0, 2.5$ . Bigger symbols correspond to larger instantons.

is usually set to larger values. To explore this further, we studied an ensemble of  $\beta = 5.7$   $6^3 \times 16$  lattices.

We followed how the wave function of a few typical very exceptional modes changed with the clover coefficient starting from the Wilson action ( $C_{sw} = 0.0$ ) up to the non-perturbatively determined value ( $C_{sw} = 2.25$ ). Ideally, we would have liked to compare the peaks of the quark density in the wave function with the instanton locations and sizes. Unfortunately, at this rather large value of

eigenvalue	location	width ( $a$ )	$\psi^\dagger\psi$ max/min
0.999	2 1 0 6	2.8	$1.8\times 10^2$
1.041	4 2 1 3	3.3	$1.4\times 10^2$
1.241	0 5 5 0	2.3	$5.3\times 10^3$
1.530	2 1 2 14	2.1	$2.1\times 10^5$
1.610	0 0 5 1	1.4	$5.8\times 10^5$

Table 1: The physical real eigenmodes of the Wilson Dirac operator ( $C_{sw} = 0.0$ ) on a typical  $\beta = 5.76^3 \times 16$  lattice. We also show the location where the quark density is peaked, the width of the peak (in lattice units) and the ratio of the maximum and minimum quark density in the given mode over the whole lattice.

the lattice spacing the instantons are quite small and the fluctuations large, so the size of the instantons is not well defined. We can still ask however how the fermions with the Wilson action “feel” whatever is left of the topology on these coarse lattices. We have therefore computed the wave function of the real modes in the physical branch with the Wilson action. For each wave function we also determined the position of the largest peak and its width. Usually the magnitude of the second largest peak was much smaller. The precise definition of the width is irrelevant here. Since we use the width only to qualitatively compare the localization of different wave functions, any sensible definition would give essentially the same results. We summarize the data for one typical configuration in Table 1.

The critical mass is  $m_c = -1.04$ , so the first mode is exceptional. The last mode in the Table is approximately halfway towards the doublers. There is a clear tendency that the quark density in modes close to  $-m_c$  has an extended broad peak and for modes towards the doublers the peaks get narrower and sharper. This is in complete agreement with [20]. Let us now follow the continuous evolution of the Wilson mode at 0.999 if the clover term is gradually turned on. Up to  $C_{sw} = 1.0$  the main peak of the quark density remains at the same location. It only slowly gets narrower: at  $C_{sw} = 1.0$  its width is 2.3. Increasing  $C_{sw}$  further, another peak appears and its relative significance increases with the clover coefficient. By  $C_{sw} = 2.25$  the wave function is completely concentrated on a very sharp peak (of width  $\approx 1$ ) located at (0 0 5 1). This is the location of the  $\lambda = 1.610$  Wilson-mode which is halfway between the doublers and  $-m_c$ . The wave function of this  $C_{sw} = 2.25$  exceptional mode is very similar to that of a Wilson mode lying halfway between the physical and the doubler branch.

We can now easily put the picture together and describe qualitatively how the exceptional modes change with the clover coefficient. The first Wilson mode can be roughly thought of as being concentrated on a single large instanton (or

instantons with roughly equal size). As the clover term is turned on, the zero modes corresponding to different instanton sizes get closer and the quark wave function spreads over several topological objects, as we also saw on the Fermilab configurations. If  $C_{sw}$  is further increased, the zero modes separate again, but this time the well localized modes (corresponding to smaller instantons) have smaller eigenvalues. The relative importance of the broader peaks decreases and the mode can become entirely concentrated on a very sharp peak. We want to emphasize however that on a given ensemble of gauge configurations at a given value of  $C_{sw}$  different (near) exceptional modes can look qualitatively very different. Some of the modes are entirely concentrated on a sharp peak — typically these are the most exceptional ones — some have several peaks of various widths. The exact picture presumably depends on the arrangement of topological objects and fluctuations on the given configuration.

The sharply peaked modes look very much like (near) doubler modes of the Wilson action and the corresponding eigenvalues and the way they change with the clover term can be very sensitive to the fluctuations on the shortest distance scale. We indeed encountered several exceptional eigenvalues at  $C_{sw} = 2.25$  (the non-perturbatively determined value) that moved anomalously quickly with the clover coefficient. This is the reason why the clover coefficient cannot be optimized to minimize the spread of the real eigenvalues.

## 4 Testing and Tuning Actions

Our goal is still to tune a clover action to have good chiral properties, i.e. to minimize the spread of the low lying modes. We see that if the clover coefficient is made too large, that program will fail. We also know from previous work [14] that an action with fat links is insensitive to short distance fluctuations, but still knows about instantons and the additional long distance behavior of the gauge field responsible for confinement. So we will begin with a fat link action of Eqn. 1. Throughout this paper we create the fat link by 10 APE smearing steps with smearing coefficient  $\alpha = 0.45$ .

Fig. 3 shows the distribution of the real eigenmodes at  $\beta = 5.8$  in terms of the bare quark mass, where the propagator is singular, for clover coefficients  $C_{sw} = 0.0$  (Wilson action),  $C_{sw} = 1.0$ ,  $C_{sw} = 1.2$  and  $C_{sw} = 1.4$ . The poles were located using the pseudoscalar density function of Eqn. 8 on 40  $8^4$  configurations. The horizontal ranges of the histograms are equal to the range the eigenmode search had been performed. To the right of the distributions is the confining phase. If one measures the pion mass in the positive mass region and extrapolates  $m_\pi^2$  to zero with the bare mass  $m_0$ , one finds that the bare mass at

which  $m_\pi = 0$  lies at a value  $m_c$  located within the range of the low-lying real eigenmodes. If a particular configuration has an eigenmode with  $m_\lambda > m_c$ , the quark propagator will be singular here. To the left of the distributions, in the negative quark mass region, are the doublers. In Fig. 3 there is no indication of them, since the doublers did not show up within the range we scanned for eigenmodes. It appears that the doublers and low lying modes are well separated at  $\beta = 5.8$ .

Using several fermion actions — all different from the one in the present paper — the authors of Ref. [20] found that real modes cover the whole investigated negative quark mass range, for all values of gauge couplings they studied, as long as the volume is large enough. Our conclusions are not in contradiction with this result. They are much more modest—that the action can be tuned to make the distribution of real eigenmodes sharply peaked near a small mean value, and that the doublers are well separated. No intrinsic property of our action protects chiral symmetry at nonzero lattice spacing and so in principle it should have real eigenmodes anywhere as well. But for practical calculations there is a big difference between a distribution with narrow peaks or a uniform spread of eigenmodes, and we are trying to construct the first kind of action.

To quantify the spread of the low energy real modes, in Fig. 4a we plot the average real eigenmode location as the function of the clover coefficient. The error bars here are not errors, they are the spread of the modes in  $m$ . Fig. 4b shows only the spread as the function of the clover coefficient.  $m_c$ , where the pion becomes massless, lies somewhere in the middle of the mode distribution, closer to its top (large mass) end. The average eigenmode locations and the upper end of the error bars in Fig. 4a bracket  $m_c$ . Smearing the link removes most of the additive mass renormalization even for the Wilson action, changing  $m_c \sim -0.95$  for the thin link action to  $m_c \sim -0.22$  for our case. Adding a clover term to the action further reduces the additive mass renormalization, and even larger clover terms induce a positive mass renormalization. At  $\beta = 5.8$  the additive mass renormalization is minimal for  $c \approx 1.2$ . This is also the value where the spread of the eigenmodes is minimal. To conclude, the results indicate that at  $\beta = 5.8$  (lattice spacing  $a \simeq 0.15$  fm) the low lying and doubler modes are well separated and explicit chiral symmetry breaking is minimized with clover coefficient  $C_{sw} = 1.2$  with our fat link action.

The situation is less convincing at  $\beta = 5.7$  (lattice spacing  $a \simeq 0.20$  fm). Fig. 5, again based on  $40 \cdot 8^4$  configurations, shows the distribution of the eigenmodes at  $\beta = 5.7$ , clover coefficient  $C_{sw} = 1.0, 1.2$  and  $1.4$ . Here the low lying modes are not as well separated as for  $\beta = 5.8$ . For  $C_{sw} = 1.0$  the distribution has a large tail extending towards negative quark masses. The situation is a bit better for  $C_{sw} = 1.2$ . Since the low lying modes are not well separated from the doublers, it makes no sense to calculate the spread of the distribution. The

continuum description of chiral symmetry breaking is about to break down at  $\beta = 5.7$ . If any of the distributions of Fig. 5 describes continuum physics, it is  $C_{sw} = 1.2$  where the overall mass renormalization is close to zero and the low lying modes are best separated from the doublers.

Finally, at  $\beta = 5.55$  (lattice spacing  $a \simeq 0.24$  fm) Fig. 6 shows that the distribution of eigenmodes is broad and the low lying modes and doublers are completely mixed.

These figures show that it is not possible to make the lattice spacing greater than about 0.2 fm, and still retain the continuum-like description of chiral symmetry breaking using a clover-like action. Other, better tuned actions might perform better at large lattice spacing. Our exploratory studies with a hypercubic fixed point [16] action showed that the FP action is not better in terms of chiral symmetry breaking than the fat link clover action with  $C_{sw} = 1.0$ . Its dispersion relation was improved at lattice spacing  $a = 0.36$  fm, and it (and the clover action) showed only a small amount of scale violation in hyperfine splittings at large lattice spacing. This just shows that scaling or near scaling of a few quantities does not guarantee that the physical mechanism responsible for chiral symmetry breaking is the same as in the continuum. This should serve as a warning sign for any calculations at large lattice spacing with actions of untested chiral properties.

In principle, one should optimize the spread not in terms of the bare quark mass, but in terms of some corresponding physical observable, like the pion mass. However, at large fattening, the relation between the bare quark mass and the pion mass shows little variation with  $C_{sw}$ .

The usual nonperturbative tuning of the clover term [22] attempts to optimize current algebra via PCAC relations. It is not clear to us how this is related to what we do, since it has been done so far only for thin link actions. We know that the optimal  $C_{sw}$  by our criterion for a thin link action is larger than the usual nonperturbative tuning, for example 2.5 vs 2.0 at  $\beta = 5.8$ . Our criterion is based on a direct attack on low energy real eigenmodes. To the extent that the dynamics of QCD for light quark masses is dominated by this physics, we feel our optimization criterion is well founded.

We do not know if there is a connection between this tuning method and the Ginsparg-Wilson [23] realization of chiral symmetry on the lattice. The free field limit of these fat link actions is identical to the standard Wilson action, and so while we are improving the chiral properties of the interacting theory, we did not improve the chiral properties of the free theory.

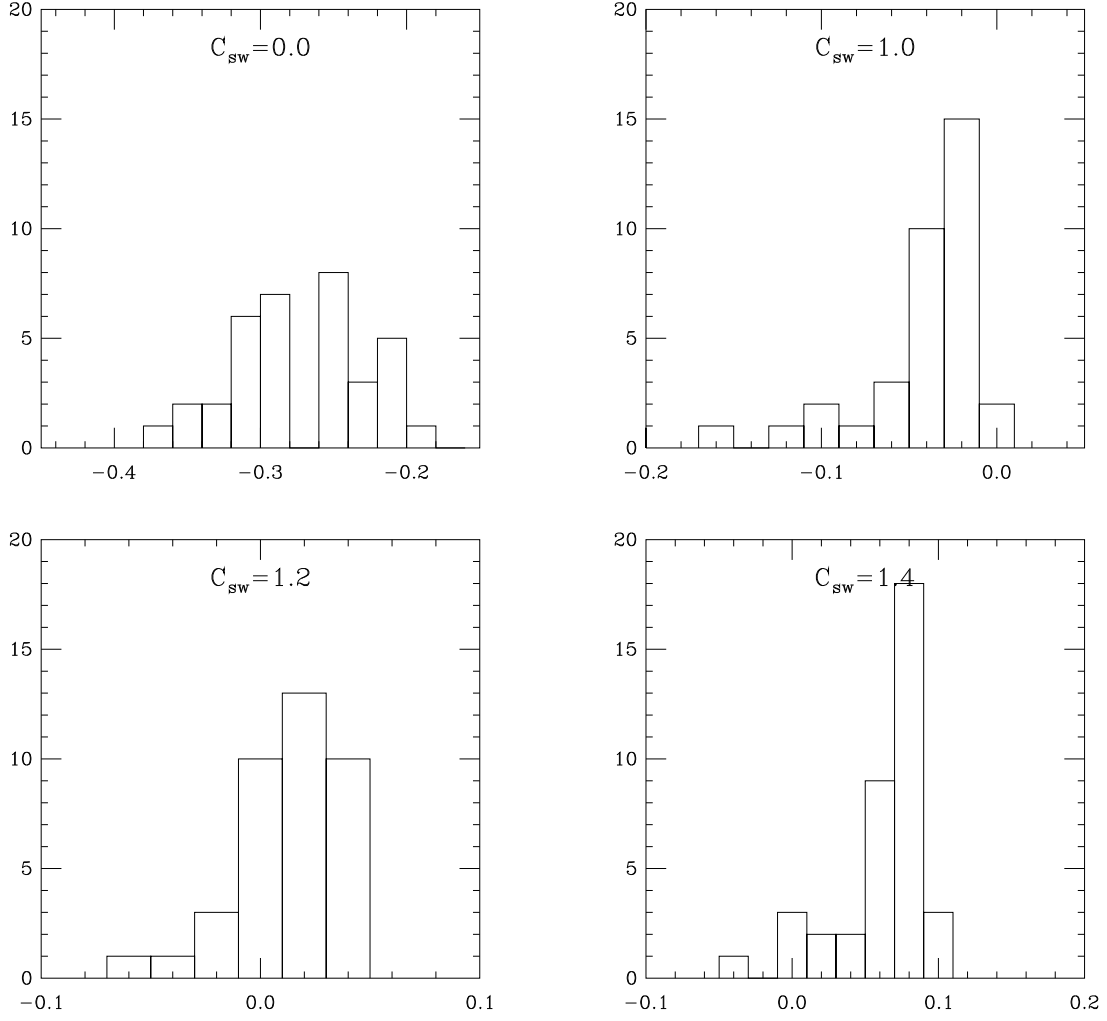


Figure 3: The distribution of the bare masses  $m$ , where the quark propagator is singular at  $\beta = 5.8$  of fat link Wilson (a); fat link clover fermions  $C_{sw} = 1.0$  (b);  $C_{sw} = 1.2$  (c);  $C_{sw} = 1.4$  (d).

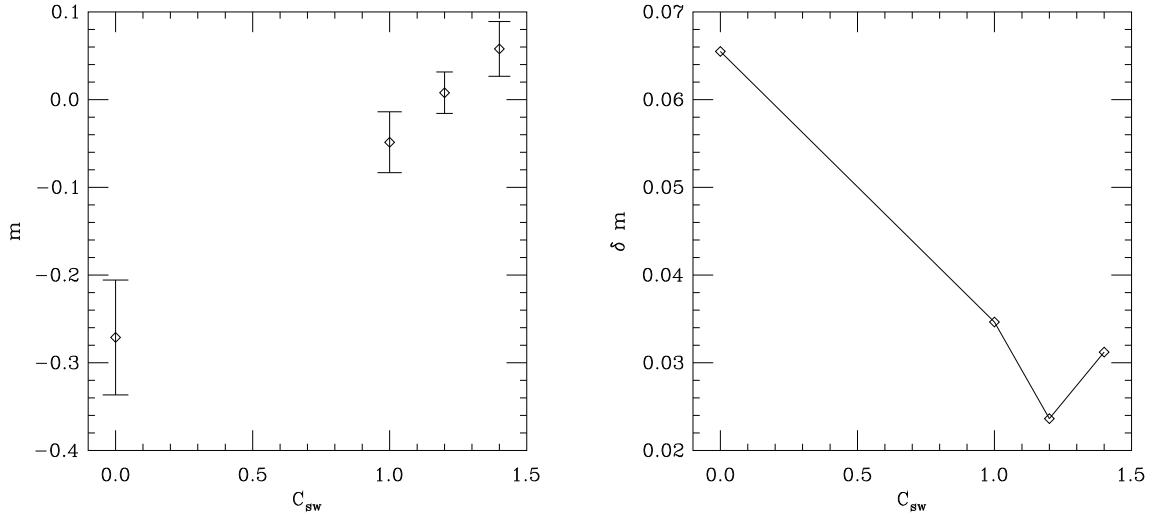


Figure 4: (a) The average real eigenmode location as the function of the clover coefficient at  $\beta = 5.8$ . The error bars show the spread of the modes. (b) The spread of the modes from (a) as the function of the clover coefficient.

## 5 Numerical Tests

We have done a calculation of spectroscopy and matrix elements at lattice spacing  $aT_c = 1/4$  ( $\beta = 5.7$  with the Wilson gauge action) using the fat link clover action with  $C_{sw} = 1.2$ , on a set of 80  $8^3 \times 24$  Wilson  $\beta = 5.7$  configurations. This is on the edge of the allowed range of lattice spacings according to our criterion of the last section. By itself, one lattice spacing is not a scaling test, but we can combine our results with those from other actions to compare the new action to them.

We expect that minimizing the spread of real eigenvalues will also improve the situation with exceptional configurations. This is indeed what happens. As a preliminary calculation, we determined all the exceptional modes on a set of 40  $6^3 \times 16$  Wilson  $\beta = 5.7$  configurations both for our optimized fat link action and the thin link clover action with  $C_{sw} = 2.25$ . The histograms of Fig. 7 show where the exceptional modes occur in terms of the lattice pion masses for both actions. For the fat link action all the modes occurred at pion masses  $m_\pi < 0.3$  which corresponds to  $m_\pi/m_\rho \leq 0.38$ , whereas the thin link clover action had five exceptional modes above  $m_\pi = 0.3$  at  $m_\pi = 0.42, 0.53, 0.39, 0.30, 0.62$  (in lattice units).

On the  $8^3 \times 24$  spectroscopy data set we only identified the eigenmodes

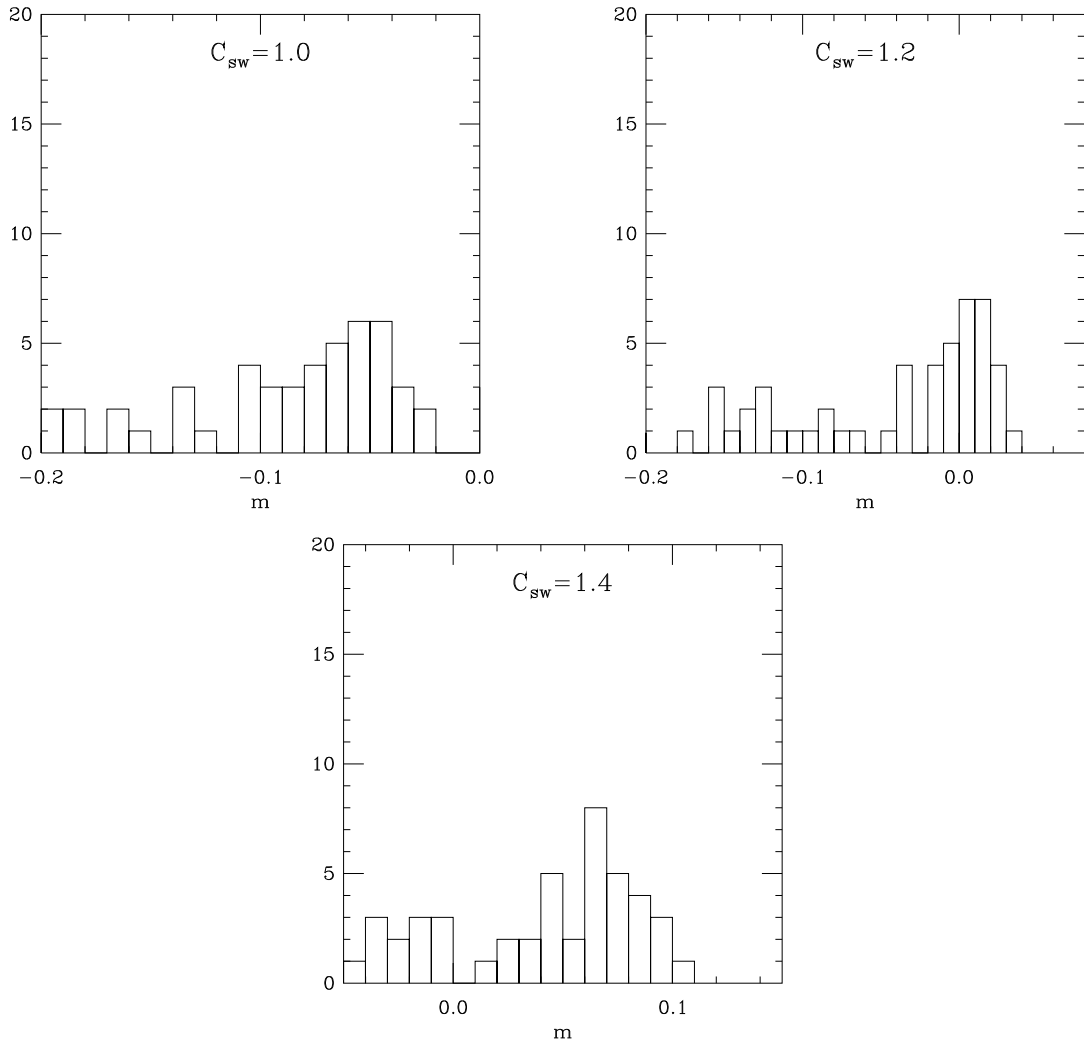


Figure 5: The distribution of the bare masses  $m$ , where the quark propagator is singular at  $\beta = 5.7$  of fat link clover fermions  $C_{sw} = 1.0$  (a);  $C_{sw} = 1.2$  (b);  $C_{sw} = 1.4$  (c).

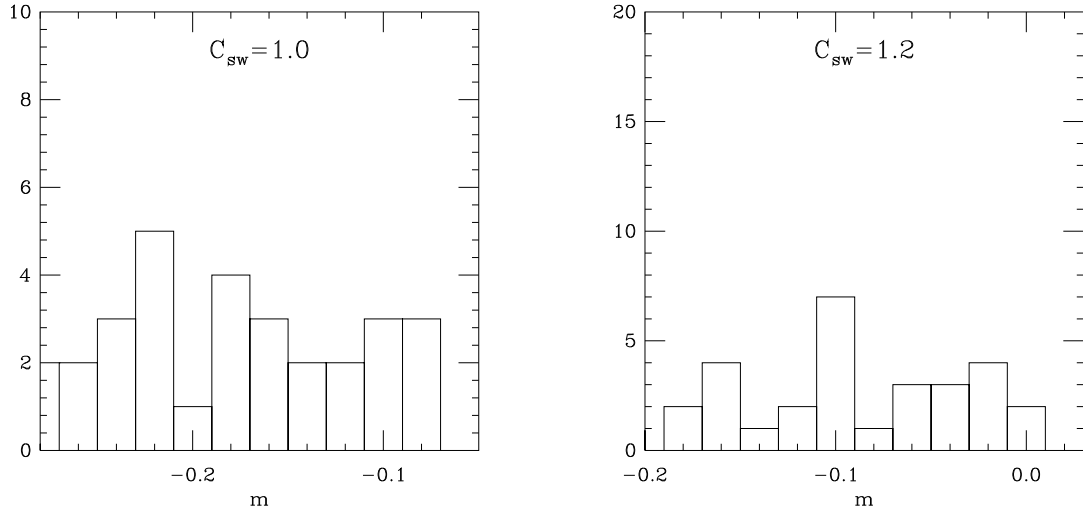


Figure 6: The distribution of the bare masses  $m$ , where the quark propagator is singular at  $\beta = 5.55$  of fat link clover fermions  $C_{sw} = 1.0$  (a);  $C_{sw} = 1.2$  (b).

occurring above  $m_\pi = 0.3$ , as going any closer to the critical mass would have been prohibitively costly. With the thin link  $C_{sw} = 2.25$  action we found 11 poles above  $m_\pi = 0.3$ , the most outlying being at  $m_\pi = 0.7$ . Using the fat link action no pole was found above  $m_\pi = 0.3$ .

We also noticed that the new action seems to be more convergent than the thin link clover action: the same biconjugate gradient code needs about half as many steps to converge to the same residue as the usual thin link clover action, for the same  $\pi/\rho$  mass ratio.

## 5.1 Spectroscopy

The spectroscopy measurement is entirely straightforward. We gauge fixed to Coulomb gauge and used a Gaussian independent particle source wave function  $\psi(r) = \exp(-(r/r_0)^2)$  with  $r_0 = 2$ . We used pointlike sinks projected onto low momentum states. We used naive currents ( $\bar{\psi}\gamma_5\psi$ , etc.) for interpolating fields. The spectra appeared to be asymptotic (as shown by good (correlated) fits to a single exponential) beginning at  $t \simeq 3 - 5$  and the best fits were selected using the HEMCGC criterion [24].

Our fiducials for comparison are Wilson action and clover action quenched spectroscopy. We have tried to restrict the data we used for comparison to

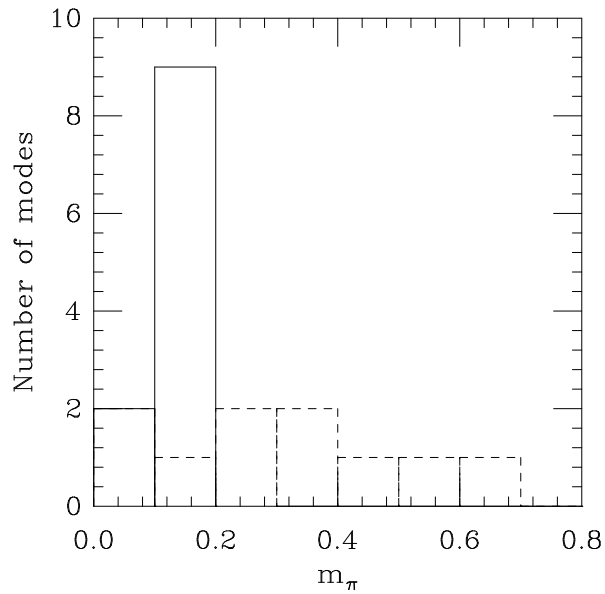


Figure 7: The distribution of exceptional fermionic modes for the thin link clover action with the non-perturbatively determined value of  $C_{sw} = 2.25$  (dashed line) and the optimized fat link action (full line). The eigenvalues are quoted in terms of the pion mass (in lattice units) where the corresponding eigenmode makes the quark propagator singular.

lattices with the proper physical volume.

We can roughly estimate the critical bare quark mass (at which the pion is massless) by linearly extrapolating  $m_\pi^2$  to zero in  $m_0$ . We also estimated the

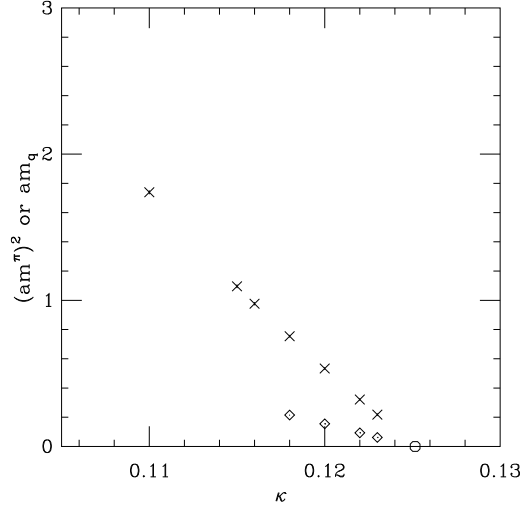


Figure 8: Bare squared pion mass (crosses) and quark mass from Eq. 12 (diamonds) vs hopping parameter for the  $C_{sw} = 1.2$  action. The octagon shows  $\kappa_c$ .

critical bare mass using the PCAC relation

$$\nabla_\mu \cdot \langle \bar{\psi} \gamma_5 \psi(0) \bar{\psi} \gamma_5 \gamma_\mu \psi(x) \rangle = 2m_q \langle \bar{\psi} \gamma_5 \psi(0) \bar{\psi} \gamma_5 \psi(x) \rangle. \quad (9)$$

which, going to the lattice and following [25], is done by fitting the pseudoscalar source-pseudoscalar sink to

$$P(t) = Z(\exp(-m_\pi t) + \exp(-m_\pi(N_t - t))) \quad (10)$$

and the pseudoscalar source-axial sink to

$$A(t) = \frac{Z_P}{Z_A} \frac{2m_q}{m_\pi} Z(\exp(-m_\pi t) - \exp(-m_\pi(N_t - t))) \quad (11)$$

to extract  $m_q$ . Fig. 8 shows the squared pion mass vs bare quark mass. The quark masses from the local pseudoscalar and axial currents are also shown.

Fits of the squared pion mass  $(am_\pi)^2 = B(1/\kappa - 1/\kappa_c)$  give  $B = 1.55(2)$  and  $\kappa_c = 0.12515(7)$ . The quark mass is fit to  $am_q = A(1/\kappa - 1/\kappa_c)$  and we find  $A = 0.447(7)$ ,  $\kappa_c = 0.12515(6)$ . In free field theory, we would expect  $A = 1/2$ ,  $\kappa_c = 1/8$ , and this is our first hint that perturbative corrections to bare quantities are small.

As a scaling test we compare  $m_\rho/T_c$  and  $m_N/T_c$  vs.  $m_\pi/T_c$  for the  $C_{sw} = 1.2$  action in Figs. 9 and 10.

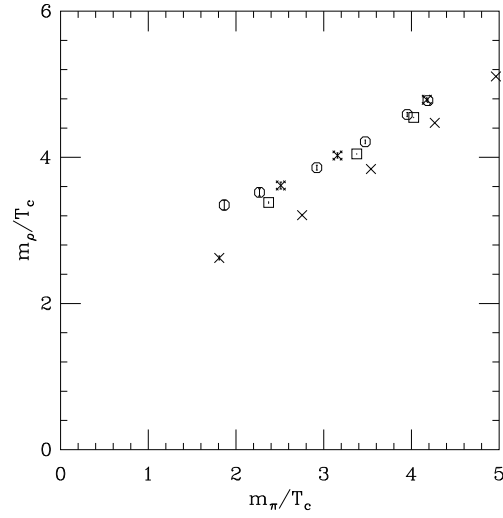


Figure 9: Octagons show  $m_\rho/T_c$  vs.  $m_\pi/T_c$  for the  $C_{sw} = 1.2$  action at  $aT_c = 1/4$ . Also shown are Wilson action data, with crosses for  $aT_c = 1/4$ , squares for  $aT_c = 1/8$ , and fancy crosses for  $aT_c = 1/12$ .

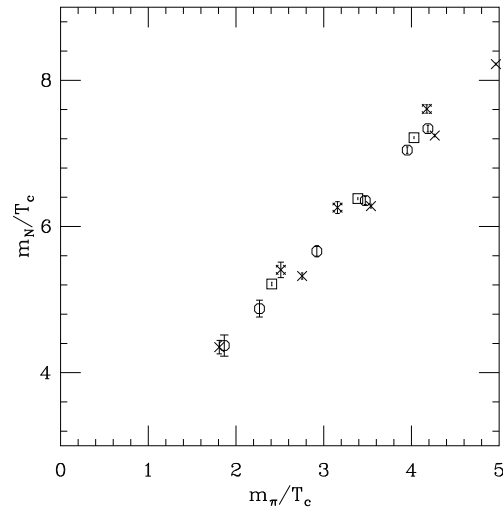


Figure 10:  $m_N/T_c$  vs.  $m_\pi/T_c$  for the  $C_{sw} = 1.2$  action and the Wilson action, labeled as in Fig. 6.

$\kappa$	PS	V	N	$\Delta$
0.118	0.868( 3)	1.053( 6)	1.589(13)	1.725(19)
0.120	0.730( 4)	0.965( 8)	1.415(19)	1.593(22)
0.122	0.567( 5)	0.880(12)	1.219(28)	1.501(24)
0.123	0.467( 6)	0.837(17)	1.093(36)	1.432(27)

Table 2: Table of best-fit masses,  $C_{sw} = 1.2$ ,  $\beta = 5.7$ .

We compare scaling violations in hyperfine splittings by interpolating our data to fixed  $\pi/\rho$  mass ratios and plotting the  $N/\rho$  mass ratio vs.  $m_\rho a$ . We do this at three  $\pi/\rho$  mass ratios, 0.80, 0.70 and 0.60, in Fig. 11. In these figures the diamonds are Wilson action data in lattices of fixed physical size,  $8^3$  at  $\beta = 5.7$  [26],  $16^3$  at  $\beta = 6.0$  [8]  $24^3$  at  $\beta = 6.3$  [27], and the crosses are data in various larger lattices:  $16^3$  and  $24^3$  at  $\beta = 5.7$  and  $32^3$  at  $\beta = 6.17$  [26],  $24^3$  at  $\beta = 6.0$  [8]. When they are present the data points from larger lattices illustrate the danger of performing scaling tests with data from different volumes. The bursts are from the nonperturbatively improved clover action of Refs. [28] and [29]. The squares show the  $C_{sw} = 1.2$  action.

We give a list of masses from the  $C_{sw} = 1.2$  action in Table 2.

We conclude that the fat link clover action has at least as good scaling behavior as the usual nonperturbatively tuned clover action.

## 5.2 Dispersion Relations

To view the dispersion relation, we first plot  $E(p)$ , the energy of the state produced with spatial momentum  $\vec{p}$ , as a function of  $|\vec{p}|$ . The result for the  $C_{sw} = 1.2$  action at  $\kappa = 0.118$  is compared to the free dispersion relation at  $aT_c = 1/4$  in Fig. 12. It looks very similar to results from the Wilson action at the same lattice spacing—an entirely unsurprising result.

This behavior is quantified by measuring the squared speed of light,  $c^2 = (E(p)^2 - m^2)/p^2$ , for  $\vec{p} = (1, 0, 0)$ . We do this by performing a correlated fit to the two propagators. The result is presented in Fig. 13 and shows the worsening of the dispersion relation at larger quark mass, characteristic Wilson/clover kinetic behavior.

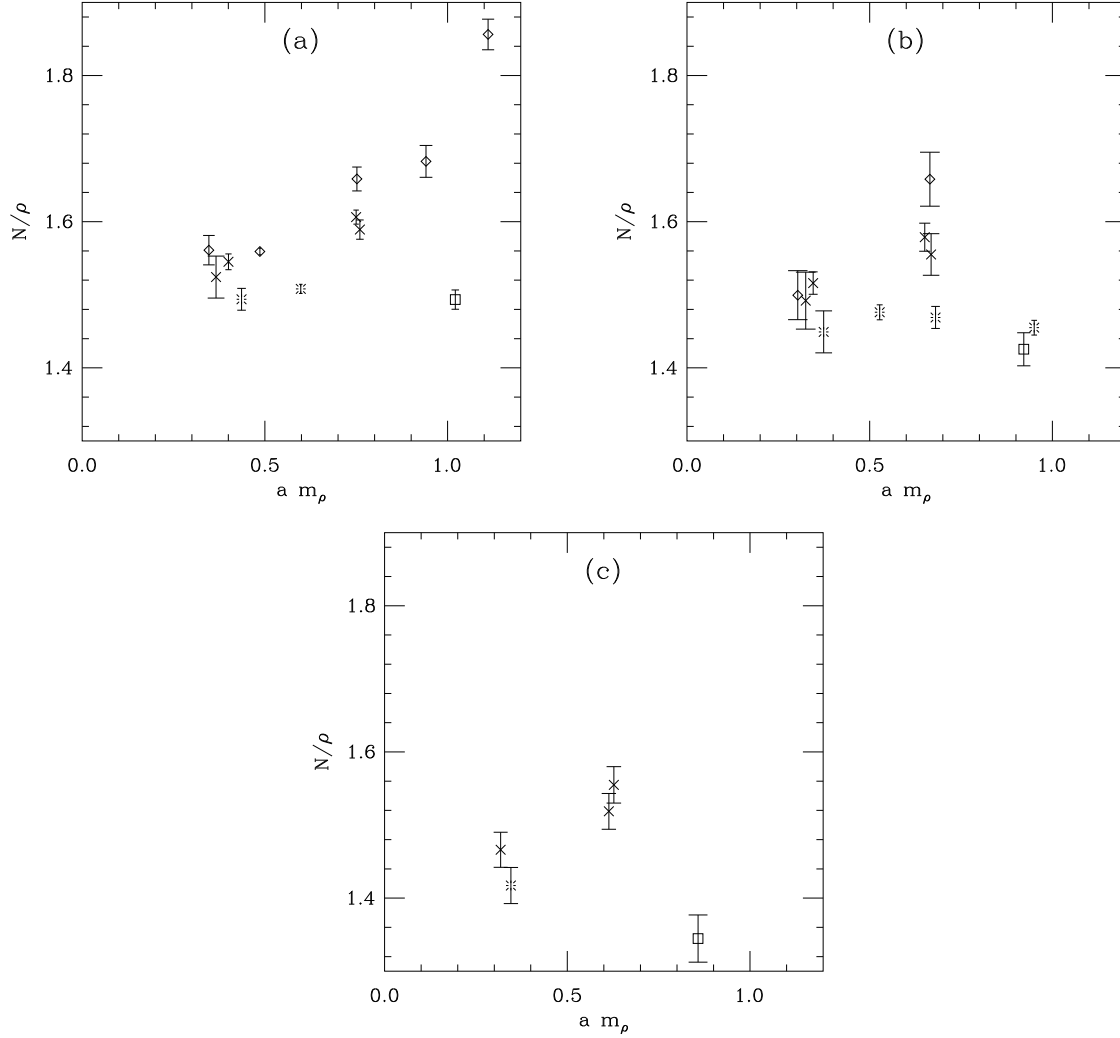


Figure 11: A scaling test for the  $C_{sw} = 1.2$  action (square) vs. Wilson actions on lattices of fixed physical size (diamonds) and larger volumes (crosses), and the nonperturbatively improved clover action (bursts). Data are interpolated to  $\pi/\rho = 0.80$  (a),  $0.70$  (b), and  $0.60$  (c).

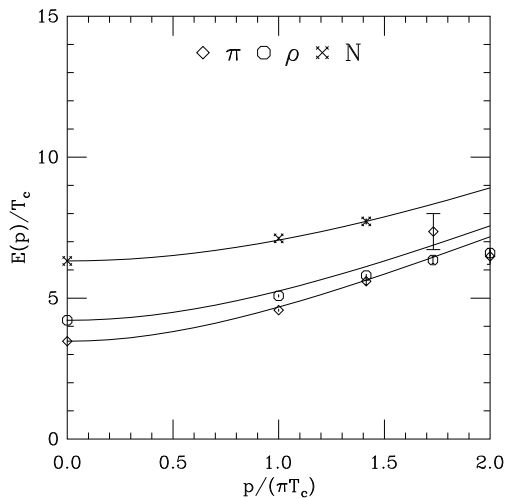


Figure 12: Dispersion relation for hadrons at  $aT_c = 1/4$  ( $a \simeq 0.18$  fm) from the  $C_{sw} = 1.2$  action. The curves are the continuum dispersion relation for the appropriate (measured) hadron mass.

### 5.3 Renormalization factors

We now turn to a (rather naive) set of measurements of simple matrix elements.

Formally, the fat link action can be regarded as “just another”  $O(a^2)$  improved action, if one assumes that the coefficient of the clover term is actually  $C_{sw} = 1 + O(g^2)$ . In perturbation theory, which involves the vector potential  $A_\mu$  rather than the link, the action shows the usual cancellation between the clover term and the scalar  $\bar{\psi}\psi A$  term. The spectrum is  $O(a^2)$ ; matrix elements using “rotated fields”  $\psi \rightarrow (1 - (\gamma \cdot D)/2)\psi$  are  $O(a^2)$  improved. Of course, the lattice-to-continuum renormalization Z-factors are different than the usual thin link clover Z-factors.

In principle, one could calculate all Z-factors using lattice perturbation theory. The Feynman rules differ from the rules for the usual clover action, only in that the vertices are multiplied by form factors, which are functions of the gluonic momentum. We have not tried to do this yet. Since we are working at fairly strong coupling, we felt that it would be easier to compute the Z-factors nonperturbatively, beginning with the vector current and then computing the axial renormalization factor using Ward identities. Since this is just the first calculation using this action, we will restrict ourselves to the naive (local) currents.

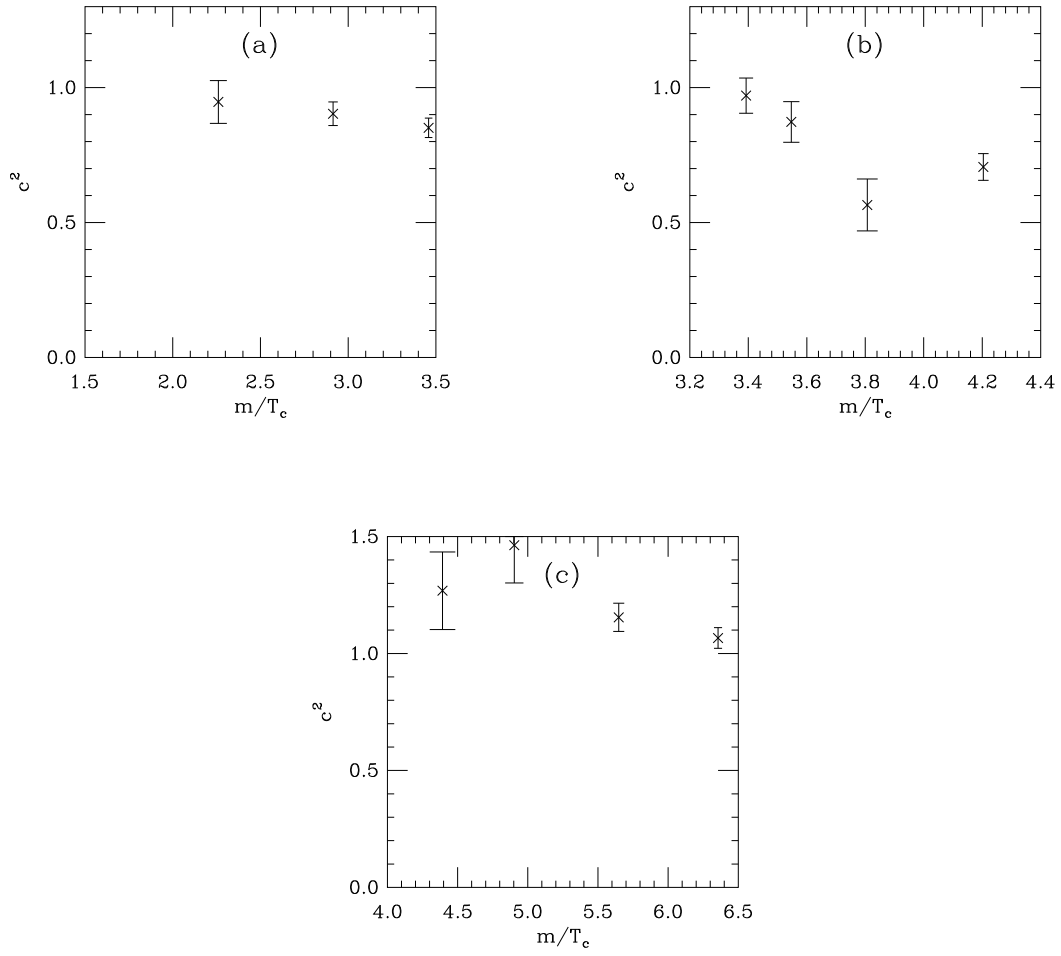


Figure 13: Squared speed of light vs. hadron mass in units of  $T_c$ , for (a) pseudoscalars, (b) vectors) and (c) protons, from the  $C_{sw} = 1.2$  action at  $\beta = 5.7$ .

We begin with the vector current. The conserved (Noether) current for the fat link action is the same as the Wilson current, just with fat links instead of thin links,

$$J_\mu^{cons}(n) = \frac{1}{2}(\bar{\psi}(n)(\gamma_\mu - 1)V_\mu(n)\psi(n + \hat{\mu}) - \bar{\psi}(n + \hat{\mu})(\gamma_\mu + 1)V_\mu^\dagger(n)\psi(n)). \quad (12)$$

This current is conserved but not improved. We choose to define the vector current Z-factor from the ratio of forward matrix elements

$$Z_V = \frac{\langle \pi(T)\pi(0) \rangle}{\langle \pi(T)J_0(t)\pi(0) \rangle} \quad (13)$$

for  $0 < t < T$ . The local current is defined as  $J_\mu^{loc}(n) = \bar{\psi}(n)\gamma_\mu\psi(n)$ . We measured the Z-factors using 20 configurations on a periodic  $8^3 \times 24$  lattice with  $T = 10$  and averaged  $9 > t > 1$ . The results of a jackknife analysis are shown in Table 3.

The fact that  $Z^{cons} \neq 1$  is a finite size effect. In the numerator of Eqn. 13 both quarks can propagate in both time directions around the torus, but the forwards and backwards paths contribute differently to the denominator. We correct this phenomenologically by computing the ratio  $Z^{loc}/Z^{cons}$  and display it in the table.

Lattice perturbation theory which correctly takes into account the residue of the pole of the massive quark[30] predicts that this ratio is equal to

$$Z_V = \frac{1 - 6\kappa}{2\kappa} \hat{Z}_V \quad (14)$$

where the  $(1 - 6\kappa)$  factor is the residue (recall  $\kappa_c = .125$ ) and  $\hat{Z}_V = 1 + ag^2 + \dots$ . As Table 3 shows, the correction to the tree level formula,  $\hat{Z}$ , which is what is usually quoted as the Z-factor, differs from unity by less than two per cent at  $\kappa = 0.123$ .

We also attempted to measure the axial vector current renormalization using the chiral Ward identity [31]. With 50 lattices, we only had a signal at  $\kappa = 0.118$ , where we found  $Z_A = 1.210(8)$ . This is again quite close to the pure kinetic result of 1.237. Dividing out the kinematic factors, this would give  $\hat{Z}_A = 0.978$ .

At  $\beta = 6.0$ , Ref. [32] found  $\hat{Z}_V = 0.824$ ,  $\hat{Z}_A = 1.09$  for the usual clover action, and improved operators.

It would be very interesting to measure the mixing of left- and right-handed operators (for  $B_K$ ) in this action.

$\kappa$	$Z^{cons}$	$Z^{loc}$	$Z^{loc}/Z^{con}$	$\frac{1-6\kappa}{2\kappa}$
0.118	1.020(1)	1.253(2)	1.228	1.237
0.120	1.032(2)	1.185(4)	1.148	1.166
0.122	1.054(5)	1.129(6)	1.071	1.098
0.123	1.071(6)	1.127(8)	1.052	1.065

Table 3: Vector current renormalization factors,  $C_{sw} = 1.2$ ,  $\beta = 5.7$ .

## 6 Conclusions

We have shown that via a combination of fattening the links and tuning the magnitude of the clover term, it is possible to optimize the chiral behavior of the clover lattice fermion action. The example we presented reduces the spread in the low energy real eigenmodes by about a factor of three in units of the squared pion mass, compared to the usual Wilson action. We fixed the fattening and varied the clover coefficient, but it is clear that a real optimization would involve varying both factors.

The same procedure can be applied to the usual clover action, without fat links. Then, the value of the clover term  $C_{sw}$  which minimizes the spread of real eigenmodes due to instantons is so large, that new kinds of configurations become exceptional. Their singular behavior is unrelated to fermion modes sitting on individual instantons. It is most likely related to short distance vacuum fluctuations. Thus this choice of action does not represent a good choice for improvement.

The method of construction exposes an apparent fundamental upper limit for the lattice spacing in a QCD simulation of about 0.2 fm. At larger lattice spacing, the doubler modes and the low energy modes do not show a clean separation, and the mechanism of chiral symmetry breaking is qualitatively different than in the continuum. The Wilson and clover actions, and the one improved action we tested, the hypercubic action of Ref. [16], failed at lattice spacing 0.24 fm. This test does not apply to actions involving heavy quarks, for which chiral symmetry is (presumably) not important, but before any other improved action can be said to reproduce continuum light hadron physics at some lattice spacing, it should show a separation between the spectrum of its near low energy modes and its doubler modes.

The “fat clover” action we have presented in this paper, as an example of an action with improved chiral properties, has many other nice properties as well. It appears to exhibit scaling of hyperfine splittings at 0.2 fm. The action is quite insensitive to the UV behavior of the underlying gauge field. It has

Z-factors for simple matrix elements which are very close to unity. And finally, the amount of resources required to construct propagators is halved compared to the usual clover action, at equivalent parameter values. It would be trivial to modify any existing clover code to improve it in the way we have described. Of course, its kinetic properties, including the dispersion relation, artifacts at large  $am_q$ , and power law scaling violations in matrix elements, are unchanged from the standard clover action's.

## Acknowledgements

We are greatly indebted to Hank Thacker who provided us the exceptional configurations reported in Ref. [6]. We would like to thank the UCLA TEP group for granting us part of the computer time used for this work. Part of the computing was done on the Origin 2000 at the University of California, Santa Barbara. This work was supported by the U.S. Department of Energy.

## References

- [1] Cf. the review talk of P. van Baal at Lattice 97, Nucl. Phys, B (Proc. Suppl.) 63 (1998) 126.
- [2] J. Negele, plenary talk at Lattice 98, hep-lat/9810053.
- [3] A. Hasenfratz and C. Nieter, hep-lat/9806026.
- [4] M. Chu, J.M. Grandy, S. Huang, and J.W. Negele, Phys. Rev. **D49** (1994) 6039, D.A. Smith, and M.J. Teper, Phys. Rev. **D58** (1998) 014505, hep-lat/9801008, P. de Forcrand, M. Garcia Perez, J.E. Hetrick, and I.O. Stamatescu, contributed to the 31st International Ahrenschoop Symposium on the Theory of Elementary Particles, Buckow, Germany, 2-6 Sep 1997; hep-lat/9802017.
- [5] Cf. D. Diakanov, Lectures at the Enrico Fermi School in Physics, Varenna, 1995, hep-ph/9602375; T. Schäfer and E. V. Shuryak, Rev. Mod. Phys. **70** (1998) 323.
- [6] W. Bardeen, A. Duncan, E. Eichten, G. Hockney and H. Thacker, Phys. Rev. **D57** (1998) 1633; W. Bardeen, A. Duncan, E. Eichten and H. Thacker, Phys. Rev. **D57** (1998) 3890; hep-lat/9606002.

- [7] P. Hasenfratz, V. Laliena and F. Niedermayer, Phys. Lett. **B427** (1998) 125, hep-lat/9801021; P. Hasenfratz, Nucl. Phys. **B525** (1998) 401, hep-lat/9802007.
- [8] M. Göckeler, et al. Phys. Lett. **B391** (1997) 388.
- [9] M. Falcioni, M. Paciello, G. Parisi, B. Taglienti, Nucl. Phys. **B251**[FS13] (1985) 624. M. Albanese, et. al. Phys. Lett. **B192** (1987) 163.
- [10] M.-C. Chu, J. M. Grandy, S. Huang and J. W. Negele, Phys. Rev. **D49** (1994) 6039.
- [11] T. Blum, et al., Phys. Rev. **D55** (1997) 1133.
- [12] K. Orginos and D. Toussaint, hep-lat/9801020.
- [13] J.-F. Lagaë and D. K. Sinclair, Nucl. Phys. B(Proc. Suppl.) 63 (1998) 892.; hep-lat/9806014.
- [14] T. DeGrand, A. Hasenfratz, T.G. Kovács, Phys. Lett. **B420** (1998) 97.
- [15] W. Bietenholz and U. J. Wiese, Nucl. Phys. **B464** (1996) 319; T. DeGrand, A. Hasenfratz, P. Hasenfratz, P. Kunszt, F. Niedermayer, Nucl. Phys. B (Proc. Suppl.) 53, 1997, 942; W. Bietenholz, et al., Nucl. Phys. B(Proc. Suppl.) 53 (1997) 921; K. Orginos, et al., hep-lat/9709100, Nucl. Phys. B (Proc. Suppl.) 63 (1998) 904; C. B. Lang and T. K. Pany, hep-lat/9707024, Nucl. Phys. **B513** (1998) 645.
- [16] T. DeGrand, Phys. Rev. **D58** (1998) 094503.
- [17] J. Smit and J. Vink, Nucl. Phys. **B286** (1987) 485, J. Vink, Nucl. Phys. **B307** (1988) 549.
- [18] H. Simma, D. Smith, Low-lying eigenvalues of the improved Wilson-Dirac operator in QCD, hep-lat/9801025.
- [19] R. G. Edwards, U. M. Heller, R. Narayanan, Nucl. Phys. **B522** (1998) 285.
- [20] R. G. Edwards, U. M. Heller, R. Narayanan, Nucl. Phys. **B535** (1998) 403, hep-lat/9802016.
- [21] H. Kluberg-Stern, A. Morel, and B. Petersson, Phys. Lett. **B114** (1982) 152.
- [22] M. Lüscher, S. Sint, R. Sommer, and P. Weisz, Nucl. Phys. **B502** (1996) 365
- [23] P. Ginsparg and K. Wilson, Phys. Rev. **D25** (1982) 2649.
- [24] K. M. Bitar, et al., Phys. Rev. **D42** (1990) 3794.

- [25] C. Bernard, et al., Phys. Rev. **D45** (1992) 3854.
- [26] F. Butler, H. Chen, J. Sexton, A. Vaccarino, and D. Weingarten, Nucl. Phys. **B430** (1994) 179.
- [27] M. Guagnelli, et al., Nucl. Phys. **B378** (1992) 616.
- [28] M. Göckeler, et. al., hep-lat/9707021, Phys. Rev. **D57** (1998) 5562.
- [29] R. G. Edwards, U. M. Heller and T. R. Klassen, Phys. Rev. Lett. **80** (1998) 3448, hep-lat/9711052.
- [30] C. Bernard, J. Labrenz, and A. Soni, Phys. Rev. **D49** (1994) 2536; G. P. Lepage and P. Mackenzie, Phys. Rev. **D48** (1993) 2250.
- [31] M. Bochicchio, et. al., Nucl. Phys. **B262** (1985) 331; L. Karsten and J. Smit, Nucl. Phys. **B183** (1981) 103. L. Maiani and G. Martinelli, Phys. Lett. **B178** (1986) 285.
- [32] G. Martinelli, S. Petrarca, C. T. Sachrajda, Phys. Lett. **B311** (1993) 241.